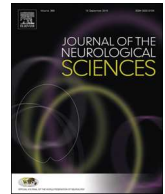




ELSEVIER

Contents lists available at ScienceDirect

Journal of the Neurological Sciences

journal homepage: www.elsevier.com/locate/jns

RP001 hydrochloride improves neurological outcome after subarachnoid hemorrhage

Ran Li^a, Poornima Venkat^b, Michael Chopp^{b,d}, Qiang Zhang^c, Tao Yan^{a,*}, Jieli Chen^{b,*}

^a Department of Neurology, Tianjin Medical University General Hospital, Tianjin Neurological Institute, Key Laboratory of Post-Neurotrauma Neurorepair and Regeneration in Central Nervous System, Ministry of Education and Tianjin City, Tianjin 300052, China

^b Neurology, Henry Ford Hospital, Detroit MI-48202, USA

^c Department of Geriatrics, Tianjin Medical University General Hospital, Tianjin 300052, China

^d Department of Physics, Oakland University, Rochester MI-48309, USA

ARTICLE INFO

Keywords:

Cardiac dysfunction
Immunoresponse
Neuroprotection
RP001 hydrochloride
Subarachnoid hemorrhage

ABSTRACT

Subarachnoid hemorrhage (SAH) results in neurological damage, acute cardiac damage and has a high mortality rate. Immunoresponse in the acute phase after SAH plays a key role in mediating vasospasm, edema, inflammation and neuronal damage. The S1P/S1PR pathway impacts multiple cellular functions, exerts anti-inflammatory and anti-apoptotic effects, promotes remyelination, and improves outcome in several central nervous system (CNS) diseases. RP001 hydrochloride is a novel S1PR agonist, which sequesters lymphocytes within their secondary tissues and prevents infiltration of immune cells into the CNS thereby reducing immune response. In this study, we investigated whether RP001 attenuates neuronal injury after SAH by reducing inflammation. S1PRs, specifically S1PR_{1,3} not only exerts anti-inflammatory effects, but also decreases heart rate and induces atrioventricular conduction abnormalities. Therefore, we also tested whether RP001 treatment of SAH regulates cardiac functional outcome. Male adult C57BL/6 mice were subjected to SAH, and neurological function tests, echocardiography, and immunohistochemical analysis were performed. SAH induces neurological deficits and acute cardiac dysfunction compared to sham control mice. Treatment of SAH with a low-dose of RP001 induces better neurological outcome and cardiac function compared to a high-dose of RP001. Low-dose-RP001 treatment significantly decreases apoptosis, white matter damage, blood brain barrier permeability, microglial/astrocyte activation, macrophage chemokine protein-1, matrix metalloproteinase-9 and NADPH oxidase-2 expression in the brain compared to SAH control mice. Our findings indicate that low-dose of RP001 alleviates neurological damage after SAH, in part by decreasing neuroinflammation.

1. Introduction

SAH (subarachnoid hemorrhage) is a devastating disease with high morbidity and mortality rate [1,2]. SAH is described as sudden blood flow into the subarachnoid space following an aneurysmal rupture or traumatic injury, leading to decreased cerebral blood flow (CBF), increased intracranial pressure (ICP), and early brain injury with pathological progression such as brain edema, inflammation, apoptosis, and oxidative stress [2,3]. Although surgical repair and some postoperative interventions may improve outcome to some extent, SAH remains a global burden and approximately 50–60% of SAH survivors suffer from residual disability [1,4]. Furthermore, there is a lack of treatments to improve neurological function after SAH [2,5,6].

Cerebral vasospasm and early brain injury are two primary reasons for SAH induced brain damage [7]. Cerebral vasospasm usually occurs

3 days after SAH [5,8], but most people die within 3 days after admission, indicating that delayed cerebral vasospasm may not be the primary cause of high mortality in the acute phase of SAH. Thus, targeting cerebral vasospasm may not be ideal to decrease mortality and improve outcome after SAH [8]. The mortality rate in the acute phase of SAH varies between 30 and 70% [8]. Recent and emerging evidence suggest that early brain injury may be a leading cause of neurological dysfunction after SAH [9]. Early brain injury occurs in the immediate period following the aneurysmal rupture, and initiates pathological cascades such as blood brain barrier (BBB) disruption, inflammation, oxidative stress, and cell death [5,10]. Immune response after SAH is a primary cause of SAH induced early brain injury. Immune cells infiltrate into the central nervous system (CNS) and interact with neurons, microglia, astrocyte, and vascular endothelium leading to CNS injury. Therefore, inhibiting immune cell infiltration after SAH may be

* Corresponding authors.

E-mail addresses: yantao78@hotmail.com (T. Yan), jieli@neuro.hfh.edu (J. Chen).

<https://doi.org/10.1016/j.jns.2019.02.005>

Received 17 September 2018; Received in revised form 1 February 2019; Accepted 4 February 2019

Available online 05 February 2019

0022-510X/ © 2019 Elsevier B.V. All rights reserved.

a viable strategy to reduce CNS injury and improve outcome [11].

Sphingosine-1-phosphate (S1P) is a biologically active metabolite formed by sphingosine kinases (SphK1 and SphK2) from sphingosine, and degraded by S1P lyase and phosphatases [12]. S1P mediates physiological processes such as maintaining BBB integrity, macrophage activation and immunocyte recruitment [11,13–15]. S1P is the phosphorylated form of sphingosine, and binds to one of 5 subtypes of S1P receptors (S1PR_{1–5}) [11]. S1PRs are G protein-coupled receptors and are widely distributed in the heart, peripheral immune system, spleen, liver and CNS [12,16]. S1PR_{1–3} can be found in the cardiac system and CNS, while there is no S1PR_{4/5} expression in the heart [17]. In humans, S1PR₁ is the primary cause for heart rate reduction and atrioventricular (AV) abnormalities, while in murine experiments, S1PR₁ and S1PR₃ are key contributors [11].

Fingolimod (FTY720), an analog of sphingosine and a non-selective agonist of S1PRs, has been approved by the Food and Drug Administration for the treatment of multiple sclerosis [11,15]. In brain hemorrhage and ischemic stroke, Fingolimod treatment can reduce neuroinflammation, neuronal death and improve neurological outcome via suppressing immune response [11,15,18,19]. Fingolimod can prevent the release of T cells and B cells from lymph nodes into peripheral blood, inhibiting their infiltration into the CNS [11]. However, numerous cardiac side effects including life-threatening bradycardia and AV block have been reported [15,20]. Fingolimod has a high affinity to S1PR₁ and S1PR₃, which may attribute to its cardiac side effects [15]. RP001 is a structural analog of Fingolimod, with similar mechanisms and pharmacological effects as Fingolimod [21], but with greater affinity for S1PR₁ and S1PR₅, and little effect on S1PR_{2,3,4} [11,21]. RP001 is a short-acting agonist of S1PR₁, which means that it can decrease S1PR₁ to undetectable levels in blood by 8 h after administration in mice and highly effective even at picomolar concentrations [22,23]. Therefore, we do not expect RP001 to have any long-term effects on S1PR₁ within the heart, and hence, minimal cardiac side effects. In this study, we investigated whether RP001 reduces SAH induced acute neurological injury and behavioral deficits via modulating immunoresponse. We also investigated whether RP001 has a dose dependent effect of neuroprotection after SAH by employing a high dose (0.5 mg/kg) and a low dose (0.3 mg/kg) treatment in an experimental SAH model in mice. In addition, we also test cardiac function using echocardiography to assess potential cardiac side effects of RP001 treatment of SAH.

2. Materials and methods

This study was conducted in accordance with the China Laboratory Animal Regulation guidelines for the use of experimental animals. Experimental protocols were approved by the Tianjin Medical University General Hospital Animal Care and Use Committee. Adequate measures were taken to minimize the number of animals used and to ensure minimal pain or discomfort in animals. Mice were maintained in a facility with a temperature-controlled environment on a 12-h light-dark cycle, and all animals were allowed free access to food and water.

2.1. SAH model

Adult, male, C57BL/6 mice (8–12 weeks old, 20–25 g) were purchased from Nanjing University. Mice were subjected to the endovascular perforation puncture SAH model as previously described [24–27]. Briefly, mice were anesthetized with 5% chloral hydrate (7 mg/kg) body weight by intraperitoneal (i.p.) injection. Core temperature was maintained at 37 °C with a homeothermic heating pad. A blunt monofilament (0.14 mm diameter, 25 mm long) was inserted through external carotid artery (ECA) into internal carotid artery (ICA). The filament was inserted along the ICA until the surgeon felt initial resistance. Then the suture was advanced approximately 1–2 mm to puncture the vessel wall and the filament was withdrawn immediately

to allow blood flow into the ventricle. The ECA was ligated, neck incision was closed and mice returned to cages to recover. Mice that were subjected to similar procedures but without puncture of the vessel wall constitute the sham control group.

2.2. Experimental groups

Mice were randomized to the following experimental groups: 1) sham control (n = 8); 2) SAH + PBS injection (n = 10); 3) SAH + low dose of RP001 treatment: SAH + 0.3 mg/kg RP001 (n = 15); 4) SAH + high dose of RP001 treatment: SAH + 0.5 mg/kg RP001 (n = 7). RP001 (TOCRIS Bioscience, United Kingdom) was administered via i.p. injection at 0.5 h, 24 h, 48 h post SAH. Mortality was calculated on the 3rd day after SAH, before sacrifice.

2.3. Neurological behavior tests

A battery of neurological function tests including the modified Garcia's score [6,28] and 100-point Katz's score [29] were conducted daily for 3 days after SAH by an investigator blinded to the experimental groups. In Garcia's score, a higher score indicates better neurological function while, in Katz's 100-point score, a lower score indicates better outcome. Only animals which had significant neurological dysfunction indicated by Garcia's score < 16 and Katz's score > 20 at day 1 after SAH were included.

2.4. Transthoracic Doppler echocardiography

Cardiac function was evaluated at 3 days after SAH by transthoracic Doppler echocardiography (VisualSonics Vevo 770, CA). Echocardiography was measured and analyzed by a professional technician who was blinded to the experimental groups. Animals were anesthetized with 3.5% isoflurane and then maintained via a facemask with 1.5% isoflurane. After shaving the thorax, ultrasound transmission gel was applied to the left chest. Left ventricular ejection fraction (LVEF), fractional shortening (FS), and heart rate were measured using two-dimensional M-mode analysis along the short axis (the level of the largest left ventricle diameter). Raw data were digitized by goal-directed, diagnostically driven software and 3 beats were averaged for each measurement.

2.5. Tissue harvest

Mice were sacrificed at 3 days after SAH. Mice were anesthetized with 10% chloral hydrate (3 mg/kg, i.p.) and placed in a supine position. Under deep anesthesia, an incision was made in the middle of their chest, and transcardially perfused with cold PBS. Then brain was immediately harvested and immersed in 4% (paraformaldehyde) for further fixation or in cold PBS for subsequent staining.

2.6. Luxol fast blue (LFB) staining

Brain coronal paraffin blocks were cut into 7 μm thin sections (bregma –1 mm to +1 mm). Brain tissue sections were deparaffinized, and rehydrated by sequential immersion in absolute, 95% and 90% ethyl alcohol. Sections were then treated with 0.1% LFB dye overnight and then with a lithium carbonate solution, aiming at color separation and making the myelin fibers appear blue and neurons appear violet. Three sections from each brain and 3 fields of view of the striatal white matter bundles were analyzed under a 20× objective of a light microscope (Olympus, Japan).

2.7. Immunofluorescent staining

Brains were fixed overnight and immersed in 15% sucrose followed by 30% sucrose. Brains were then embedded using O.C.T. Compound

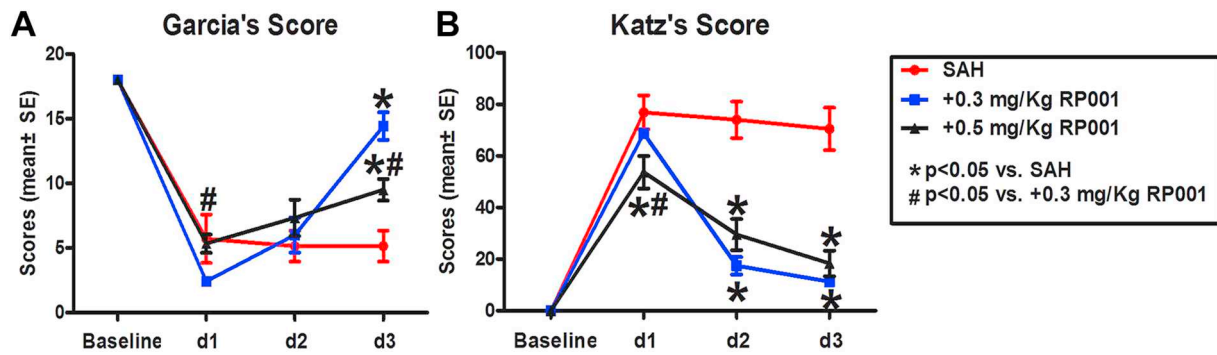


Fig. 1. Both high and low dose RP001 treatment significantly improves neurological functional outcome after SAH in mice.

A: Both high dose RP001 (0.5 mg/kg) and low dose RP001 (0.3 mg/kg) treatment of SAH significantly alleviates neurological functional deficits compared to SAH control mice as indicated by Garcia's score ($p < .05$). In addition, low dose RP001 significantly improves neurological function compared to high dose RP001 treatment measured by Garcia's score ($p < .05$). B: Both high dose and low dose RP001 treatment of SAH significantly alleviates neurological functional deficits compared to SAH control group as indicated by the Katz's score ($p < .05$).

embedding medium (Sakura, USA). Frozen brain coronal tissue were cut into 8 μm thick sections (from bregma -1 mm to $+1$ mm) and immunofluorescence staining was performed [30]. The tissue was equilibrated at room temperature for at least 30 min. Then the slides were permeabilized with cold acetone for 20 min at -20°C , and washed three times with cold PBS for 5 min. Brain slides were incubated with 3% BSA (bovine serum) in PBS for 1 h at room temperature. Primary antibody against MCP-1 (macrophage chemokine protein-1, a macrophage chemokine protein, Rat monoclonal IgG, 1:200, Abcam), NOX-2 (NADPH oxidase-2, component of membrane-bound oxidase and generate superoxide, Rabbit polyclonal IgG, 1:250, Abcam), IBA-1 (marker of microglia, Goat polyclonal IgG, 1:500, Abcam), GFAP (glial fibrillary acidic protein, marker of astrocytes, Rabbit polyclonal IgG, 1:500, Abcam), MMP-9 (matrix metalloproteinase-9, marker of extracellular matrix breakdown, mouse monoclonal, 1:500, Santa Cruz Biotechnology), albumin (marker of BBB disruption, rabbit monoclonal, 1:250, Abcam) diluted with 3% BSA. Overnight incubation with primary antibody was performed. The slides were washed 3 times with cold PBS for 10 min. Fluorophore conjugated secondary antibody, AF488 donkey anti-Rat (1:500, Invitrogen, Life Technologies), AF488 goat anti-Rabbit (1:500, Invitrogen, Life Technologies), AF546 donkey anti-Goat (1:500, Invitrogen, Life Technologies), AF488 donkey anti-mouse (1:500, Invitrogen, Life Technologies), were diluted with PBS and incubated for 1 h at room temperature. Slides were then counterstained with DAPI (diamidino phenylindole, nuclear staining, Abcam), mounted with a compatible mounting medium and cover slipped. Three slides from each brain and 4 fields of view from striatum and cortex were analyzed under a $20\times$ objective of a fluorescence microscope (Olympus, Japan).

2.8. TUNEL assay

Frozen tissue was prepared as described above. TUNEL (Roche, Germany) staining was used to detect apoptosis [30]. Tissue was equilibrated at room temperature for at least 30 min. Slides were then permeabilized with cold acetone for 20 min at -20°C , and washed three times with cold PBS for 5 min. TUNEL working solution was applied following manufacturer's guidelines for 1 h at room temperature. Slides were counterstained with DAPI and cover slipped. Three slides from each brain and 4 fields of view from striatum and cortex were analyzed under a $20\times$ objective of a fluorescence microscope (Olympus, Japan).

2.9. Quantification

Data were analyzed by a technician who was blind to the experimental groups. Image-Pro Plus 6.0 software was used for

immunostaining analysis. For TUNEL immunostaining, the number of positively labeled cells was counted. For all other immunostaining, the data are quantified as density of positive immunolabeling. For each field of view, the positive stained area was measured using built-in densitometry function with a density threshold above the unstained set uniformly for all groups. Data were averaged to obtain a single value for each animal and presented as either number of positive cells/area in mm^2 or as percentage positive area.

2.10. Statistical analysis

Difference in mortality rate between SAH and SAH + 0.3 mg/kg RP001 group was analyzed by Chi-Square test. All data were normally distributed and the homogeneity of variances was tested. Differences measured from two functional tests at each time point, LFB and immunostaining analysis were analyzed by one-way analysis of variance (ANOVA) as appropriate using Graphpad Prism 5.0 software. All values are expressed as mean \pm SE (standard error), p values $< .05$ are considered statistically significant.

3. Results

3.1. Treatment of SAH with RP001 significantly improves neurological outcome

Mice subjected to SAH and treated with either high or low dose RP001 exhibit significantly improved neurological function compared to SAH control mice, identified by higher Garcia's score and lower Katz's score ($p < .05$, Fig. 1A–B). Garcia's score also indicates that SAH mice treated with low dose RP001 exhibit improved neurological functional recovery compared to SAH mice treated with high dose RP001 ($p < .05$, Fig. 1A). However, there were no significant differences between high and low dose RP001 treated SAH mice in Katz's score ($p > .05$, Fig. 1B). No animals died in the sham control group. Mortality rates were not significantly different among SAH (20%, 2 of 10 mice died), SAH + 0.3 mg/kg RP001 (26.7%, 4 of 15 mice died) and SAH + 0.5 mg/kg RP001 (14.3%, 1 of 7 mice died) groups.

3.2. Treatment of SAH with RP001 does not induce evident adverse cardiac side effects, while low dose RP001 increases heart rate

To test whether RP001 induces cardiac deficits after SAH, echocardiography was performed at 3 days after SAH. Fig. 2 shows that SAH significantly induces cardiac deficits identified by decreased LVFS, LVEF, and decreased heart rate compared to sham control mice ($p < .05$). Compared to sham control mice, both SAH mice treated with low or high dose RP001 do not exhibit significant cardiac deficits

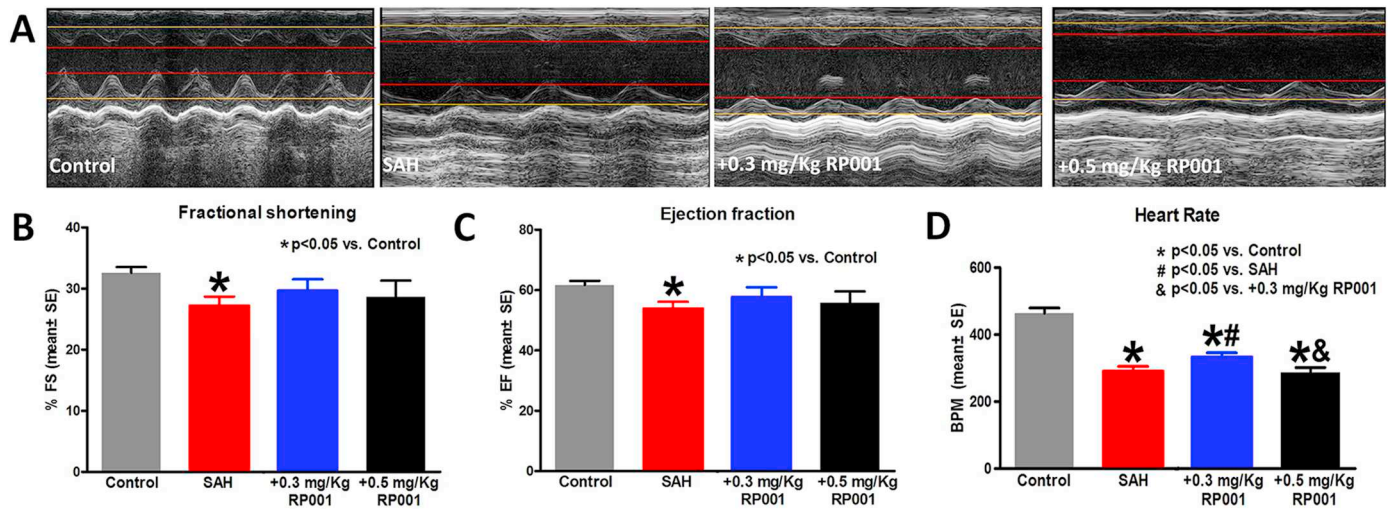


Fig. 2. Low dose RP001 treatment of SAH in mice significantly improves heart rate without aggravating cardiac function compared to non treated SAH mice or SAH mice receiving high dose RP001 treatment.

A: Representative images of M-mode echocardiography result in sham control, SAH control, low dose RP001 (0.3 mg/kg) and high dose RP001 (0.5 mg/kg) treated SAH mice. B-D: SAH significantly induces cardiac deficits indicated by decreased FS, EF and heart rate compared to sham control mice. Both low and high dose RP001 treatment of SAH in mice do not influence FS or EF compared to SAH or sham control mice ($p > .05$), but significantly decrease heart rate compared to sham control mice ($p < .05$). In addition, low dose RP001 treatment significantly increases heart rate ($p < .05$) compared to SAH control as well as high dose RP001 treated SAH mice.

identified by LVFS and LVEF. SAH mice with or without RP001 treatment exhibit significantly decreased heart rate compared to sham control mice. Low dose RP001 treated mice exhibit significantly increased heart rate compared to the SAH (non treated) group as well as high dose RP001 treated mice. However, high dose RP001 treatment failed to increase heart rate compared to SAH mice. The data indicate that SAH treatment with both doses of RP001 significantly improves neurological functional outcome without aggravating cardiac dysfunction. Low dose RP001 treatment induces improved neurological functional outcome measured by Garcia's score and increases heart rate after SAH in mice compared to SAH mice receiving high dose RP001 treatment. Therefore, we focus on low dose of RP001 treatment for immunostaining analysis.

3.3. RP001 treatment decreases apoptosis, white matter damage and BBB disruption after SAH

To investigate whether low dose RP001 treatment of SAH in mice induces neuroprotection, TUNEL staining was used to evaluate neuronal apoptosis. Fig. 3A–B shows that SAH significantly increases apoptosis in the brain compared to sham control mice. Low dose RP001 treatment significantly reduces apoptosis in the brain compared to the SAH control group ($p < .05$, $n = 6$ /group).

To test whether RP001 induces white matter damage, LFB staining was performed [31]. Fig. 3C–D shows that SAH significantly decreases myelin density in the striatum compared to sham control mice. RP001 treatment significantly increases myelin density in the striatum compared to non-treated SAH control mice ($p < .05$, $n = 6$ /group).

To test if RP001 treatment of SAH protects the BBB, immunofluorescence staining against albumin was performed. Fig. 3E–F shows that SAH significantly increases BBB leakage identified by increased albumin density in the brain compared to sham control mice, while RP001 treatment significantly reduces BBB breakdown compared to SAH control mice ($p < .05$, $n = 6$ /group). These data indicate that SAH increases apoptosis, white matter damage and BBB leakage, while RP001 treatment reduces apoptosis, white matter damage and BBB disruption after SAH.

3.4. RP001 treatment reduces immunoresponse and oxidative stress after SAH

To test whether RP001 treatment affects immunoresponse and oxidative stress after SAH, we employed immunofluorescence to measure MCP-1, MMP-9 and NOX-2 expression in the brain. SAH significantly increases MCP-1, MMP-9 and NOX-2 expression in the brain compared to sham control mice. RP001 treatment of SAH significantly decreases the expression of MCP-1 (Fig. 4A–B), MMP-9 (Fig. 4C–D) and NOX-2 (Fig. 4E–F) in the brain compared with the non-treated SAH control group ($p < .05$, $n = 6$ /group). The data indicate that RP001 treatment of SAH significantly reduces neuroinflammation and oxidative stress in the brain compared to SAH control mice.

3.5. RP001 treatment reduces SAH induced microglial and astrocyte activation

Microglia and activated astrocytes are the major resident macrophages in the CNS [30,32]. In addition, immune cell infiltration can also activate astrocytes [33]. To test whether RP001 treatment reduces the resident glial cell immunoresponse, IBA-1 and GFAP immunofluorescent staining were performed. Fig. 5A–D shows that SAH significantly increases the activation of microglia (A–B) and astrocytes (C–D) compared to sham control mice. RP001 treatment of SAH significantly decreases activation of microglia (A–B) and astrocytes (C–D) compared to non-treated SAH control mice ($p < .05$, $n = 6$ /group). The data indicate that low dose RP001 treatment decreases microglial and astrocyte activation compared with the SAH group.

4. Discussion

This is the first study to investigate the therapeutic effects of RP001 treatment in the acute phase of SAH in mice. We report that low dose RP001 treatment of SAH improves neurological function, decreases white matter damage, BBB leakage, immune response, and oxidative stress in the brain, while increasing heart rate compared with SAH mice. High dose RP001 also significantly improved neurological function compared to sham SAH mice; however, low dose treatment significantly improved Garcia's score compared to high dose RP001

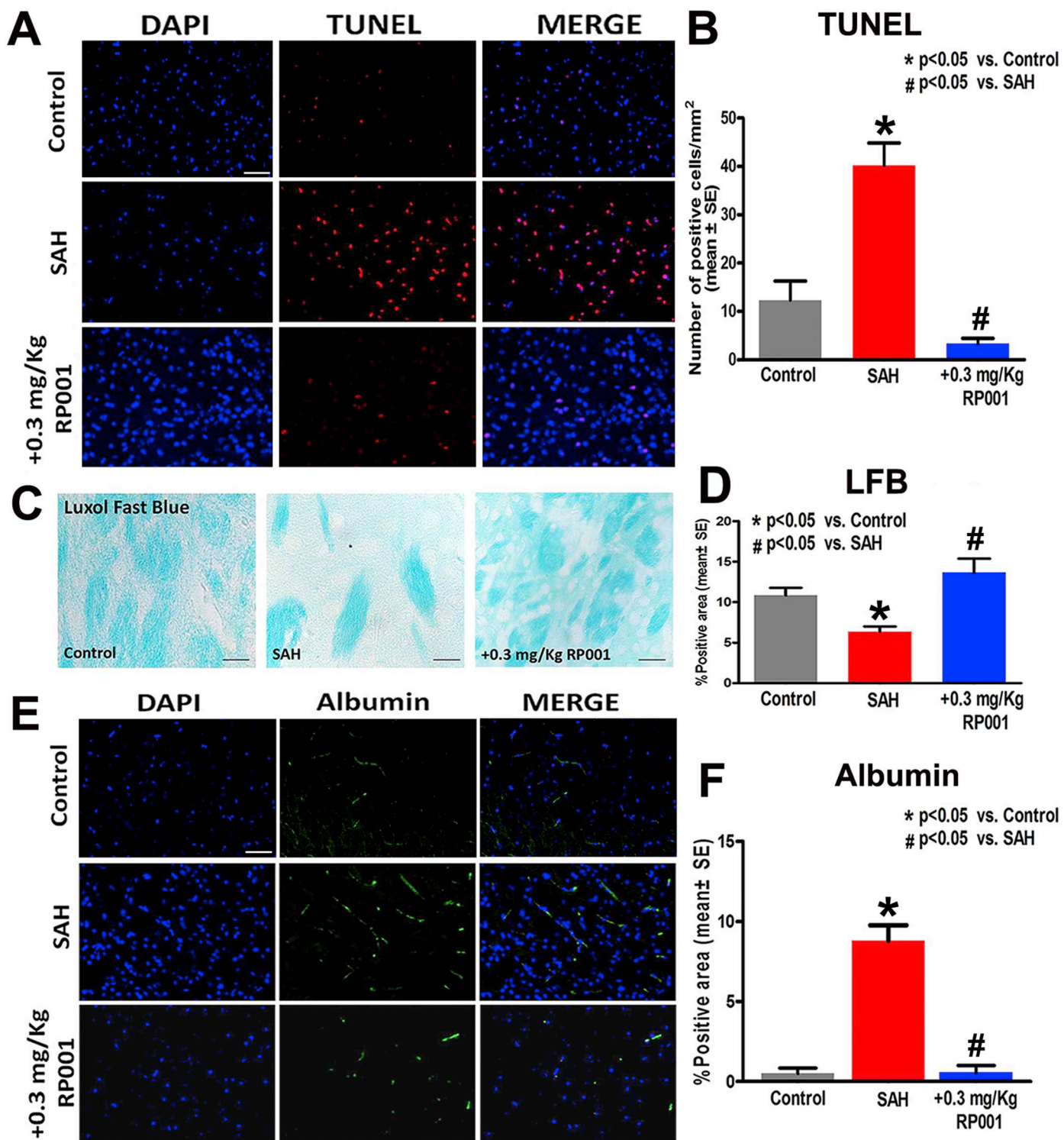
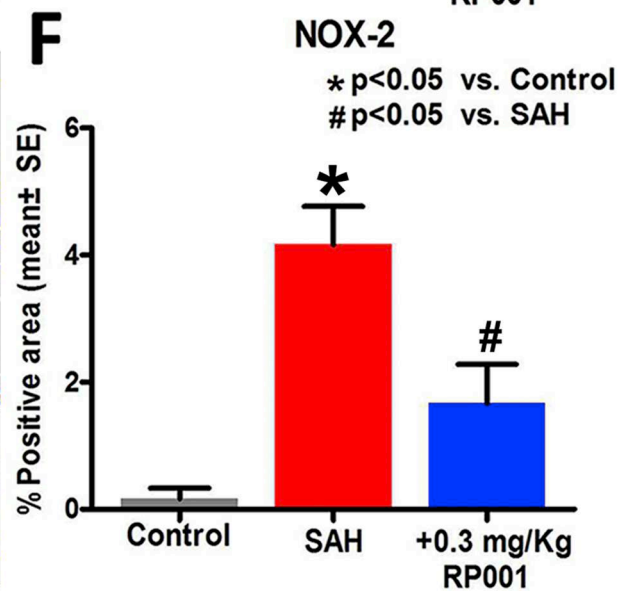
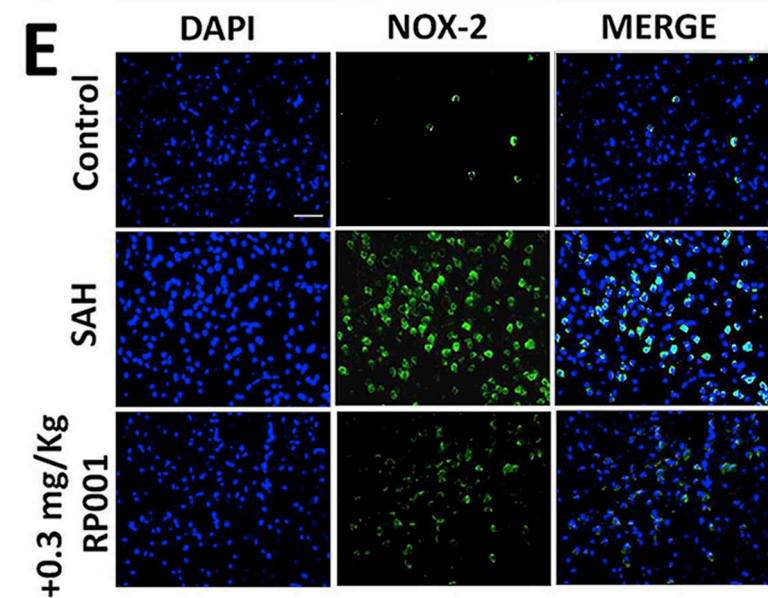
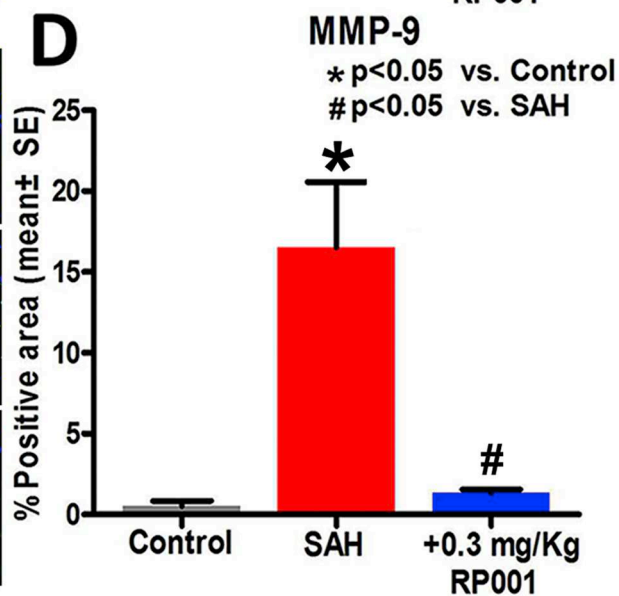
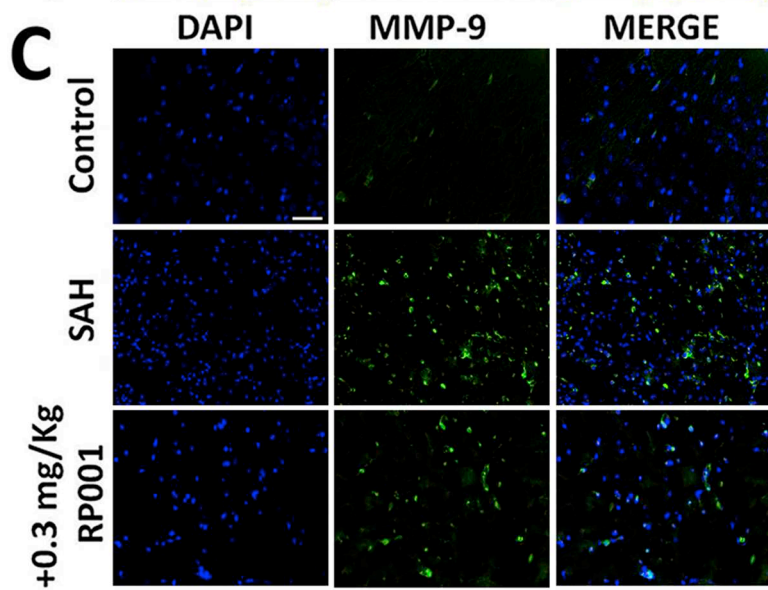
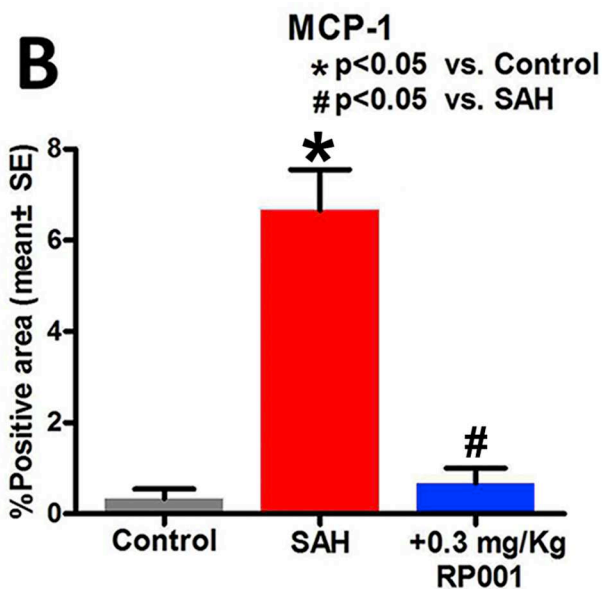
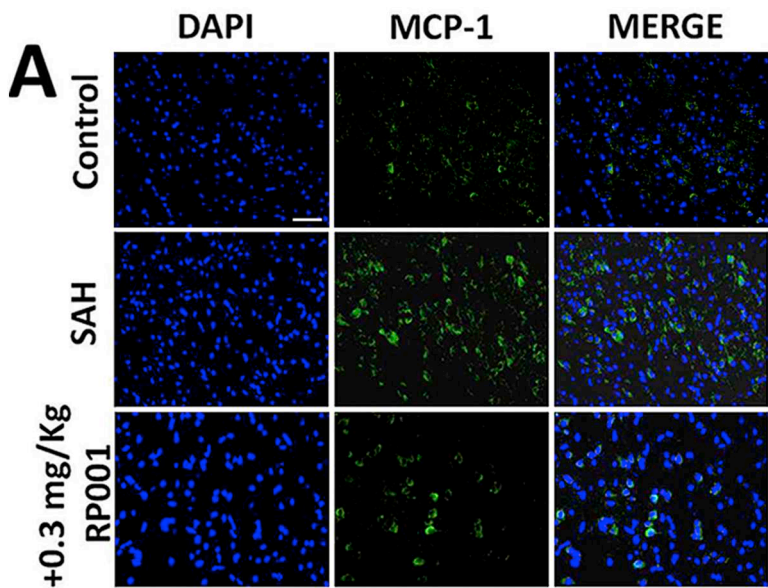


Fig. 3. Low dose RP001 treatment of SAH in mice significantly decreases apoptosis, white matter damage and BBB disruption compared to SAH control mice. A–B: Representative images and quantitative data show that SAH significantly increases neuronal apoptosis in the brain compared to sham control mice, while low dose RP001 (0.3 mg/kg) treatment significantly decreases apoptosis compared to SAH control mice, as indicated by TUNEL immunostaining. Scale bar: 100 μm, *p < .05 vs. Control, #p < .05 vs. SAH. C–D: Representative images and quantitative data showing that SAH significantly decreases myelin density in the striatal white matter bundles compared to sham control mice, while low dose RP001 treatment significantly increases myelin density compared to SAH control mice, indicated by Luxol fast blue (LFB) immunostaining. Scale bar: 20 μm, *p < .05 vs. Control, #p < .05 vs. SAH. E–F: Representative images and quantitative data showing that SAH significantly increases BBB leakage compared to sham control mice, while low dose RP001 treatment significantly decreases BBB leakage compared to SAH control mice, indicated by albumin immunostaining. Scale bar: 100 μm, *p < .05 vs. Control, #p < .05 vs. SAH.

treatment. In addition, high dose RP001 treated SAH group exhibited a significant heart rate reduction compared with the low dose RP001 treated SAH group. Thus, low dose RP001 treatment of SAH was further

studied.

SAH not only induces neurological deficits, but also increases cardiac dysfunction. Cardiac dysfunction, which includes



(caption on next page)

Fig. 4. Low dose RP001 treatment of SAH in mice significantly reduces inflammation and oxidative stress compared to SAH control mice. Representative images and quantitative data show that SAH significantly increases inflammatory factors MCP-1 (A–B) and MMP-9 (C–D), as well as oxidative stress marker NOX-2 (E–F) compared to sham control mice. Low dose RP001 (0.3 mg/kg) treatment of SAH significantly decreases MCP-1, MMP-9 and NOX-2 expression in the brain compared to SAH control mice. Scale bar: 100 μ m, *p < .05 vs. Control, #p < .05 vs. SAH.

electrocardiogram abnormalities, cardiac arrhythmia, Takotsubo cardiomyopathy and myocardial enzyme changes, are common after SAH [4,34]. In this study, we found that SAH significantly induces cardiac deficits identified by decreased LVFS, LVEF and heart rate compared to sham control mice. Low dose RP001 treatment of SAH significantly improves neurological outcome and heart rate without cardiac side effects. The mechanisms underlying low dose RP001 induced heart rate improvement are not clear. A potential mechanism may be attributed to observation that S1PR₁₋₃ is strongly expressed in cardiomyocytes, while very low levels of S1PR₄ and S1PR₅ are detected in the heart tissue [16,36]. RP001 has a primary affinity to S1PR₁ and S1PR₅, but not S1PR₃, which is the main cause for heart rate reduction, AV conduction disturbances and sinus bradycardia [21,37]. Therefore, there are no

apparent significant cardiac side effects following low or high dose RP001 treatment of SAH in mice. Low dose RP001 treatment results in better heart rate than high dose RP001 treatment which may be due to 2 factors: firstly, since RP001 is highly potent with low IC₅₀ values for S1PR₁, and moderate affinity for S1PR₅ and little affinity for S1PR₂₋₄, non-specific or off-target binding may occur at high dose RP001 [22]. Secondly, compared to high dose, low dose RP001 may have a reduced effect on S1PR₁, which is known to affect cardiac contractility and heart rate [36]. Previous studies have found that inflammation mediates brain-heart interaction after stroke and brain injury (). Stroke increases inflammatory cell infiltration into heart and promotes circulating inflammatory factor expression which may induce cardiac deficits (). Anti-inflammation may reduce stroke induced heart damage. RP001

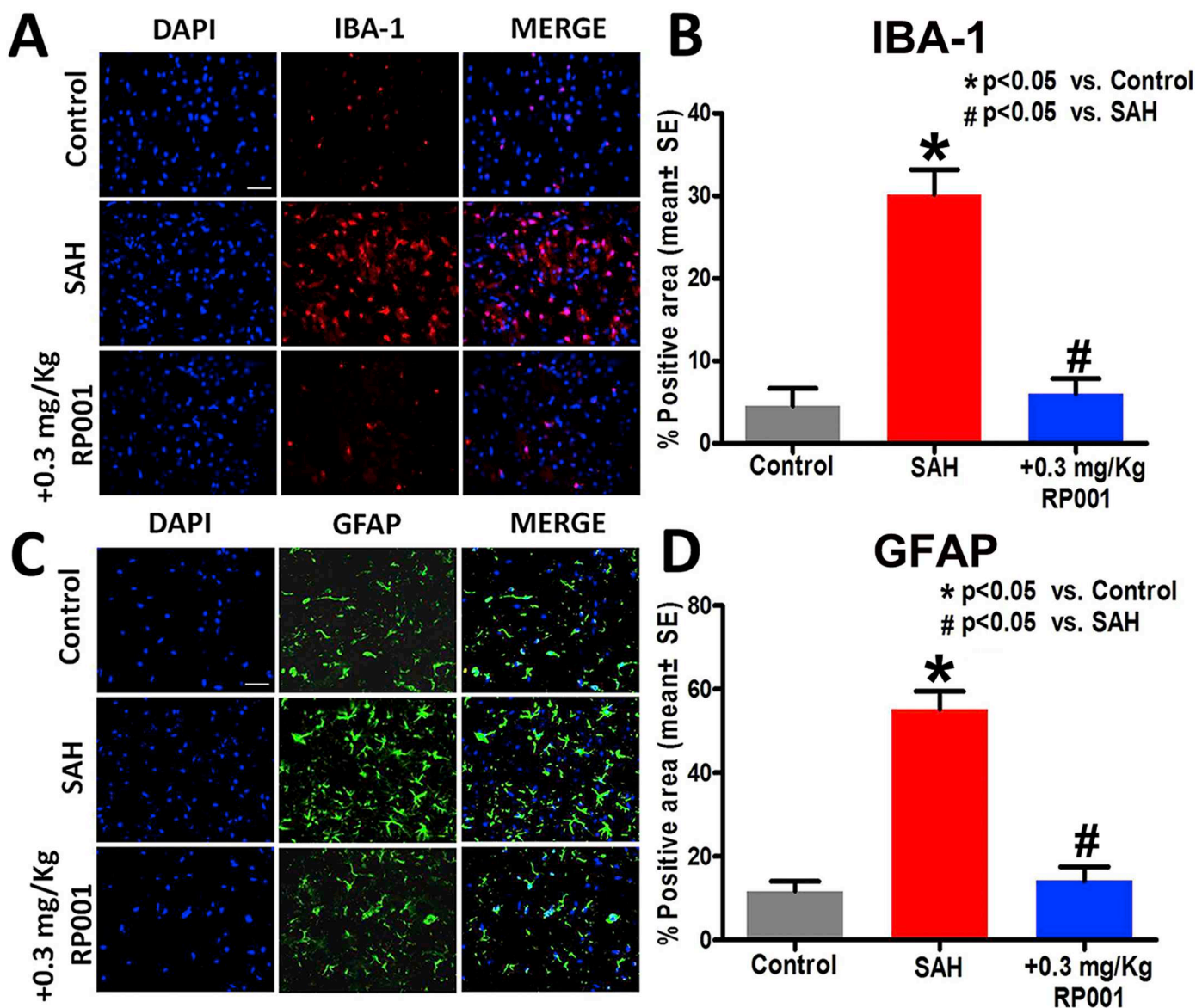


Fig. 5. Low dose RP001 treatment of SAH reduces microglial and astrocyte activation compared to SAH control mice. Representative images and quantitative data showing that SAH significantly increases microglia marker IBA-1 expression (A–B) and astrocyte marker GFAP expression (C–D) compared to sham control mice, while low dose RP001 (0.3 mg/kg) treatment significantly decreases IBA-1 and GFAP positive immunolabeling compared to SAH control mice. Scale bar: 100 μ m, *p < .05 vs. Control, #p < .05 vs. SAH.

has anti-inflammatory effects which may also play a role in RP001 induced heart rate improvement after SAH. However, the mechanisms by which RP001 mediates heart function warrant further investigation.

Many clinical trials aiming at reducing cerebral vasospasm after SAH have failed [38]. To date, Nimodipine, the most commonly used vasodilator, is employed to treat SAH via lowering intracranial pressure [5,8,39]. Clazosentan can decrease vasospasm after SAH, but does not significantly improve neurological injury and mortality rate [2,4,40]. RP001 has a primary affinity to S1PR₁ and S1PR₅, but less affinity to S1PR₂₋₄. Also, S1PR_{1-3, 5} is present in the CNS but S1PR₄ is lacking [41]. S1PR₁ is expressed by neurons, oligodendrocytes, astrocytes, microglia and endothelial cells, and plays a key role in neurite extension and retraction, myelinogenesis, astrogliosis and microglial activation [41]. S1PR₅ is highly expressed on endothelial cells within the BBB [42,43]. S1PR₅ decreases transendothelial migration of monocytes, and by decreasing the activation of NFκB, S1PR₅ reduces downstream leukocyte adhesion molecules and inflammatory chemokines and cytokines [43]. S1PR₅ is also expressed on oligodendrocytes, mediates oligodendrocyte differentiation and survival and thereby influences neuronal myelination processes [44,45]. CNS inflammation is known to induce neuronal apoptosis, demyelination, oxidative response, inflammatory factor expression and activation of microglia and astrocytes [11]. Microglia are the primary resident macrophages in the CNS, and serve as the first-line of immune defense in the CNS [39,46]. Importantly, activated microglia release a large number of pro-inflammatory cytokines which may aggravate brain injury [46]. Activated microglia also stimulate astrocytes to secrete pro-inflammatory factors [47]. S1PRs activate neuro-inflammatory responses and regulate astrogliosis [48]. RP001 can induce internalization of S1PRs, primarily S1PR₁ and S1PR₅ [21]. Internalization of S1PRs leads to decrease of CNS inflammation, BBB disruption, and apoptosis [11]. In this study, we found that low dose RP001 treatment not only decreases microglial activation, but also decreases activation of astrocytes, promotes remyelination and decreases apoptosis as well as improves functional outcome after SAH.

Immune response is rapidly triggered upon aneurysm rupture [9], and inflammation plays an important role both in early [9] and delayed brain injury [49]. After SAH, pro-inflammatory cytokines are released into serum and cerebrospinal fluid (CSF) causing early brain injury, delayed vasospasm and long-term neurological deficits [8,9,40]. MCP-1 is an important inflammatory factor that mediates monocyte migration and infiltration, as well as activation of memory T lymphocytes and natural killer (NK) cells [50]. MCP-1 is highly expressed in aneurysms but is not present in normal arteries, and MCP-1 is closely related to CNS immunoresponse [50,51]. CSF and serum levels of MCP-1 significantly correlate to long-term neuroinflammation, cerebral vasospasm, and poor clinical grades after SAH [50–52]. Some studies show that expression of MCP-1 is elevated on days 1–5 after SAH, with peak expression on day 3 and decline after day 5 [50]. Oxidative response occurs early after SAH, and causes brain injury such as vascular smooth cell and endothelium damage, BBB disruption, vasospasm, and apoptosis, all of which contribute to poor prognosis [8,33]. NOX-2, often referred to as, phagocytic NOX, has a high expression in neurons, phagocytes and astrocytes [33,53]. NOX-2 plays a crucial role in early brain injury after SAH [54]. Our data show that SAH increases the expression of MCP-1 and NOX-2, and RP001 treatment of SAH significantly decreases MCP-1 and NOX-2 expression after SAH. In addition, RP001 treatment also suppresses inflammation and apoptosis.

Protecting the integrity of the BBB is a crucial factor which affects severity of brain injury and prognosis of SAH [14]. Brain edema following BBB disruption leads to increased severity of brain injury [55]. Inflammation and neuronal apoptosis contribute to BBB leakage [17]. Endothelial cells in the CNS highly express S1PRs [17]. Increased MMP-9 expression is typically associated with aggravated BBB damage in most cerebrovascular diseases including SAH [11,55]. Preventing/minimizing BBB disruption after SAH may have therapeutic effects such as improved neurological outcome [55]. In this study, we found that

RP001 treatment significantly decreases MMP-9 expression and decreases BBB leakage after SAH. It is likely that RP001 improves BBB integrity and decreases inflammatory response as well as promotes neuronal remyelination which may in concert contribute to improved functional outcome after SAH.

5. Conclusions

Low dose RP001 treatment following SAH in mice significantly decreases immune response and oxidative stress in the brain, improves neurological function, and alleviates early brain injury without inducing cardiac side effects. Alleviating neuroinflammation may be an important target for SAH treatment in the acute phase.

Acknowledgements

The authors wish to thank Yahui Wan and Shanshan Cao for their technical assistance.

Sources of funding

This work was supported by the National Key R&D Program of China 2017YFC1308401, the National Natural Science Foundation of China grant 81771277, 81571145, 81671144, 91746205, Tianjin Natural Science Foundation Grant 17JCZDJC36100.

Conflict of interest

The authors state that they have no conflicts of interest to disclose.

References

- [1] R.E. Ayer, R.P. Ostrowski, T. Sugawara, Q. Ma, N. Jafarian, J. Tang, J.H. Zhang, Statin-induced T-lymphocyte modulation and neuroprotection following experimental subarachnoid hemorrhage, *Acta Neurochir. Suppl.* 115 (2013) 259–266, https://doi.org/10.1007/978-3-7091-1192-5_46.
- [2] S. Chen, H. Wu, J. Tang, J. Zhang, J.H. Zhang, Neurovascular events after subarachnoid hemorrhage: focusing on subcellular organelles, *Acta Neurochir. Suppl.* 120 (2015) 39–46, https://doi.org/10.1007/978-3-319-04981-6_7.
- [3] R. Ayer, W. Chen, T. Sugawara, H. Suzuki, J.H. Zhang, Role of gap junctions in early brain injury following subarachnoid hemorrhage, *Brain Res.* 1315 (2010) 150–158, <https://doi.org/10.1016/j.brainres.2009.12.016>.
- [4] S. Chen, Q. Li, H. Wu, P.R. Krafft, Z. Wang, J.H. Zhang, The harmful effects of subarachnoid hemorrhage on extracerebral organs, *Biomed. Res. Int.* 2014 (2014) 858496, <https://doi.org/10.1155/2014/858496>.
- [5] M. Fujii, J. Yan, W.B. Rolland, Y. Soejima, B. Caner, J.H. Zhang, Early brain injury, an evolving frontier in subarachnoid hemorrhage research, *Transl. Stroke Res.* 4 (4) (2013) 432–446, <https://doi.org/10.1007/s12975-013-0257-2>.
- [6] P. Sherchan, T. Lekic, H. Suzuki, Y. Hasegawa, W. Rolland, K. Duris, Y. Zhan, J. Tang, J.H. Zhang, Minocycline improves functional outcomes, memory deficits, and histopathology after endovascular perforation-induced subarachnoid hemorrhage in rats, *J. Neurotrauma* 28 (12) (2011) 2503–2512, <https://doi.org/10.1089/neu.2011.1864>.
- [7] H. Suzuki, Y. Hasegawa, W. Chen, K. Kanamaru, J.H. Zhang, Recombinant osteopontin in cerebral vasospasm after subarachnoid hemorrhage, *Ann. Neurol.* 68 (5) (2010) 650–660, <https://doi.org/10.1002/ana.22102>.
- [8] F.A. Sehba, R.M. Pluta, J.H. Zhang, Metamorphosis of subarachnoid hemorrhage research: from delayed vasospasm to early brain injury, *Mol. Neurobiol.* 43 (1) (2011) 27–40, <https://doi.org/10.1007/s12035-010-8155-z>.
- [9] S. Chen, Q. Ma, P.R. Krafft, Q. Hu, W. Rolland 2nd, P. Sherchan, J. Zhang, J. Tang, J.H. Zhang, P2X7R/cryopyrin inflammasome axis inhibition reduces neuroinflammation after SAH, *Neurobiol. Dis.* 58 (2013) 296–307, <https://doi.org/10.1016/j.nbd.2013.06.011>.
- [10] M. Fujii, P. Sherchan, Y. Soejima, Y. Hasegawa, J. Flores, D. Doycheva, J.H. Zhang, Cannabinoid receptor type 2 agonist attenuates apoptosis by activation of phosphorylated CREB-Bcl-2 pathway after subarachnoid hemorrhage in rats, *Exp. Neurol.* 261 (2014) 396–403, <https://doi.org/10.1016/j.expneurol.2014.07.005>.
- [11] V. Brinkmann, A. Billich, T. Baumruker, P. Heining, R. Schmouder, G. Francis, S. Aradhye, P. Burtin, Fingolimod (FTY720): discovery and development of an oral drug to treat multiple sclerosis, *Nat. Rev. Drug Discov.* 9 (11) (2010) 883–897, <https://doi.org/10.1038/nrd3248>.
- [12] C. Wang, J. Mao, S. Redfield, Y. Mo, J.M. Lage, X. Zhou, Systemic distribution, subcellular localization and differential expression of sphingosine-1-phosphate receptors in benign and malignant human tissues, *Exp. Mol. Pathol.* 97 (2) (2014) 259–265, <https://doi.org/10.1016/j.yexmp.2014.07.013>.
- [13] O. Altay, Y. Hasegawa, P. Sherchan, H. Suzuki, N.H. Khatibi, J. Tang, J.H. Zhang,

- Isoflurane delays the development of early brain injury after subarachnoid hemorrhage through sphingosine-related pathway activation in mice, *Crit. Care Med.* 40 (6) (2012) 1908–1913, <https://doi.org/10.1097/CCM.0b013e3182474bc1>.
- [14] O. Altay, H. Suzuki, Y. Hasegawa, B. Caner, P.R. Krafft, M. Fujii, J. Tang, J.H. Zhang, Isoflurane attenuates blood-brain barrier disruption in ipsilateral hemisphere after subarachnoid hemorrhage in mice, *Stroke* 43 (9) (2012) 2513–2516, <https://doi.org/10.1161/STROKEAHA.112.661728>.
- [15] M.G. Sanna, J. Liao, E. Jo, C. Alfonso, M.Y. Ahn, M.S. Peterson, B. Webb, S. Lefebvre, J. Chun, N. Gray, H. Rosen, Sphingosine 1-phosphate (S1P) receptor subtypes S1P1 and S1P3, respectively, regulate lymphocyte recirculation and heart rate, *J. Biol. Chem.* 279 (14) (2004) 13839–13848, <https://doi.org/10.1074/jbc.M311743200>.
- [16] N. Ahmed, D. Linardi, I. Decimo, R. Mehboob, M.A. Gebrie, G. Innamorati, G.B. Luciani, G. Faggian, A. Rungtatscher, Characterization and expression of sphingosine 1-phosphate receptors in human and rat heart, *Front. Pharmacol.* 8 (2017) 312, <https://doi.org/10.3389/fphar.2017.00312>.
- [17] L. Fan, H. Yan, FTY720 attenuates retinal inflammation and protects blood-retinal barrier in diabetic rats, *Invest. Ophthalmol. Vis. Sci.* 57 (3) (2016) 1254–1263, <https://doi.org/10.1167/iovs.15-18658>.
- [18] C.A. Huppe, P. Blais Lecours, A. Lechasseur, D.R. Gendron, A.M. Lemay, E.Y. Bissonnette, M.R. Blanchet, C. Duchaine, M.C. Morissette, H. Rosen, D. Marsolais, A sphingosine-1-phosphate receptor 1 agonist inhibits tertiary lymphoid tissue reactivation and hypersensitivity in the lung, *Mucosal Immunol.* 11 (1) (2018) 112–119, <https://doi.org/10.1038/mi.2017.37>.
- [19] J. Zhang, Z.G. Zhang, Y. Li, X. Ding, X. Shang, M. Lu, S.B. Elias, M. Chopp, Fingolimod treatment promotes proliferation and differentiation of oligodendrocyte progenitor cells in mice with experimental autoimmune encephalomyelitis, *Neurobiol. Dis.* 76 (2015) 57–66, <https://doi.org/10.1016/j.nbd.2015.01.006>.
- [20] S. Feiler, B. Friedrich, K. Scholler, S.C. Thal, N. Plesnila, Standardized induction of subarachnoid hemorrhage in mice by intracranial pressure monitoring, *J. Neurosci. Methods* 190 (2) (2010) 164–170, <https://doi.org/10.1016/j.jneumeth.2010.05.005>.
- [21] S.M. Cahalan, P.J. Gonzalez-Cabrera, G. Sarkisyan, N. Nguyen, M.T. Schaeffer, L. Huang, A. Yeager, B. Clemons, F. Scott, H. Rosen, Actions of a picomolar short-acting S1P(1) agonist in S1P(1)-eGFP knock-in mice, *Nat. Chem. Biol.* 7 (5) (2011) 254–256, <https://doi.org/10.1038/nchembio.547>.
- [22] S.M. Cahalan, P.J. Gonzalez-Cabrera, G. Sarkisyan, N. Nguyen, M.-T. Schaeffer, L. Huang, A. Yeager, B. Clemons, F. Scott, H. Rosen, Actions of a picomolar short-acting S1P₁ agonist in S1P₁-eGFP knock-in mice, *Nat. Chem. Biol.* 7 (5) (2011) 254–256, <https://doi.org/10.1038/nchembio.547>.
- [23] M. Kono, E.G. Conlon, S.Y. Lux, K. Yanagida, T. Hla, R.L. Proia, Bioluminescence imaging of G protein-coupled receptor activation in living mice, *Nat. Commun.* (2017) 1163.
- [24] D. Buhler, K. Schuller, N. Plesnila, Protocol for the induction of subarachnoid hemorrhage in mice by perforation of the Circle of Willis with an endovascular filament, *Transl. Stroke Res.* 5 (6) (2014) 653–659, <https://doi.org/10.1007/s12975-014-0366-6>.
- [25] E. Kooijman, C.H. Nijboer, C.T. van Velthoven, A. Kavelaars, J. Kesecioglu, C.J. Heijnen, The rodent endovascular puncture model of subarachnoid hemorrhage: mechanisms of brain damage and therapeutic strategies, *J. Neuroinflammation* 11 (2014) 2, <https://doi.org/10.1186/1742-2094-11-2>.
- [26] J.B. Bederson, I.M. Germano, L. Guarino, Cortical blood flow and cerebral perfusion pressure in a new noncraniotomy model of subarachnoid hemorrhage in the rat, *Stroke* 26 (6) (1995) 1086–1091 (discussion 1091–2).
- [27] J. Wang, X. Fu, C. Jiang, L. Yu, M. Wang, W. Han, L. Liu, J. Wang, Bone marrow mononuclear cell transplantation promotes therapeutic angiogenesis via upregulation of the VEGF-VEGFR2 signaling pathway in a rat model of vascular dementia, *Behav. Brain Res.* 265 (2014) 171–180, <https://doi.org/10.1016/j.bbr.2014.02.033>.
- [28] N. Turan, B.A. Miller, R.A. Heider, M. Nadeem, I. Sayeed, D.G. Stein, G. Pradilla, Neurobehavioral testing in subarachnoid hemorrhage: a review of methods and current findings in rodents, *J. Cereb. Blood Flow Metab.* 37 (11) (2017) 3461–3474, <https://doi.org/10.1177/0271678X16665623>.
- [29] H. Jeon, J. Ai, M. Sabri, A. Tariq, X. Shang, G. Chen, R.L. Macdonald, Neurological and neurobehavioral assessment of experimental subarachnoid hemorrhage, *BMC Neurosci.* 10 (2009) 103, <https://doi.org/10.1186/1471-2202-10-103>.
- [30] T. Tamura, M. Aoyama, S. Ukai, H. Kakita, K. Sobue, K. Asai, Neuroprotective erythropoietin attenuates microglial activation, including morphological changes, phagocytosis, and cytokine production, *Brain Res.* 1662 (2017) 65–74, <https://doi.org/10.1016/j.brainres.2017.02.023>.
- [31] C.Y. Xia, S. Zhang, Y. Gao, Z.Z. Wang, N.H. Chen, Selective modulation of microglia polarization to M2 phenotype for stroke treatment, *Int. Immunopharmacol.* 25 (2) (2015) 377–382, <https://doi.org/10.1016/j.intimp.2015.02.019>.
- [32] S. Liebner, R.M. Dijkhuizen, Y. Reiss, K.H. Plate, D. Agalliu, G. Constantin, Functional morphology of the blood-brain barrier in health and disease, *Acta Neuropathol.* 135 (3) (2018) 311–336, <https://doi.org/10.1007/s00401-018-1815-1>.
- [33] X. Shi, Y. Fu, S. Zhang, H. Ding, J. Chen, Baicalin attenuates subarachnoid hemorrhagic brain injury by modulating blood-brain barrier disruption, inflammation, and oxidative damage in mice, *Oxidative Med. Cell. Longev.* 2017 (2017) 1401790, <https://doi.org/10.1155/2017/1401790>.
- [34] R.I. Lowensohn, M. Weiss, E.H. Hon, Heart-rate variability in brain-damaged adults, *Lancet* 1 (8012) (1977) 626–628.
- [35] C.K. Means, J.H. Brown, Sphingosine-1-phosphate receptor signalling in the heart, *Cardiovasc. Res.* 82 (2) (2009) 193–200, <https://doi.org/10.1093/cvr/cvp086>.
- [36] M.G. Sanna, K.P. Vincent, E. Repetto, N. Nguyen, S.J. Brown, L. Abgaryan, S.W. Riley, N.B. Leaf, S.M. Cahalan, W.B. Kioussis, Y. Kohno, J.H. Brown, A.D. McCulloch, H. Rosen, P.J. Gonzalez-Cabrera, Bitopic sphingosine 1-phosphate receptor 3 (S1P3) antagonist rescue from complete heart block: pharmacological and genetic evidence for direct S1P3 regulation of mouse cardiac conduction, *Mol. Pharmacol.* 89 (1) (2016) 176–186, <https://doi.org/10.1124/mol.115.100222>.
- [37] F. Al-Mufti, K. Amuluru, B. Smith, N. Damodara, M. El-Ghanem, I.P. Singh, N. Dangayach, C.D. Gandhi, Emerging markers of early brain injury and delayed cerebral ischemia in aneurysmal subarachnoid hemorrhage, *World Neurosurg.* 107 (2017) 148–159, <https://doi.org/10.1016/j.wneu.2017.07.114>.
- [38] Y. Chen, Q. Li, J. Tang, H. Feng, J.H. Zhang, The evolving roles of pericyte in early brain injury after subarachnoid hemorrhage, *Brain Res.* 1623 (2015) 110–122, <https://doi.org/10.1016/j.brainres.2015.05.004>.
- [39] R.P. Ostrowski, J.H. Zhang, Hyperbaric oxygen for cerebral vasospasm and brain injury following subarachnoid hemorrhage, *Transl. Stroke Res.* 2 (3) (2011) 316–327, <https://doi.org/10.1007/s12975-011-0069-1>.
- [40] S. O'Sullivan, K.K. Dev, Sphingosine-1-phosphate receptor therapies: advances in clinical trials for CNS-related diseases, *Neuropharmacology* 113 (Pt B) (2017) 597–607, <https://doi.org/10.1016/j.neuropharm.2016.11.006>.
- [41] A.D. Hobson, C.M. Harris, E.L. van der Kam, S.C. Turner, A. Abibi, A.L. Aguirre, P. Bousquet, T. Kebede, D.B. Konopacki, G. Gintant, Y. Kim, K. Larson, J.W. Maull, N.S. Moore, D. Shi, A. Shrestha, X. Tang, P. Zhang, K.K. Sarris, Discovery of A-971432, an orally bioavailable selective sphingosine-1-phosphate receptor 5 (S1P5) agonist for the potential treatment of neurodegenerative disorders, *J. Med. Chem.* 58 (23) (2015) 9154–9170, <https://doi.org/10.1021/acs.jmedchem.5b00928>.
- [42] R. van Doorn, M.A. Lopes Pinheiro, G. Kooij, K. Lakeman, B. van het Hof, S.M. van der Pol, D. Geerts, J. van Horssen, P. van der Valk, E. van der Kam, E. Ronken, A. Reijerkerk, H.E. de Vries, Sphingosine 1-phosphate receptor 5 mediates the immune quiescence of the human brain endothelial barrier, *J. Neuroinflammation* 9 (2012) 133, <https://doi.org/10.1186/1742-2094-9-133>.
- [43] C. Jaillard, S. Harrison, B. Stankoff, M.S. Aigrot, A.R. Calver, G. Duddy, F.S. Walsh, M.N. Pangalos, A. Arimura, K. Kaibuchi, B. Zalc, C. Lubetzki, Edg8/S1P5: an oligodendroglial receptor with dual function on process retraction and cell survival, *J. Neurosci.* 25 (6) (2005) 1459–1469, <https://doi.org/10.1523/jneurosci.4645-04.2005>.
- [44] H. Mattes, K.K. Dev, R. Bouhelal, C. Barske, F. Gasparini, D. Guerini, A.K. Mir, D. Orain, M. Osinde, A. Picard, C. Dubois, E. Tasdelen, S. Haessig, Design and synthesis of selective and potent orally active S1P5 agonists, *ChemMedChem* 5 (10) (2010) 1693–1696, <https://doi.org/10.1002/cmdc.201000253>.
- [45] S. Wei, C. Luo, S. Yu, J. Gao, C. Liu, Z. Wei, Z. Zhang, L. Wei, B. Yi, Erythropoietin ameliorates early brain injury after subarachnoid haemorrhage by modulating microglia polarization via the EPOR/JAK2-STAT3 pathway, *Exp. Cell Res.* 361 (2) (2017) 342–352, <https://doi.org/10.1016/j.yexcr.2017.11.002>.
- [46] Y. Shinozaki, K. Shibata, K. Yoshida, E. Shigetomi, C. Gachet, K. Ikenaka, K.F. Tanaka, S. Koizumi, Transformation of astrocytes to a neuroprotective phenotype by microglia via P2Y1 receptor downregulation, *Cell Rep.* 19 (6) (2017) 1151–1164, <https://doi.org/10.1016/j.celrep.2017.04.047>.
- [47] S.S. Dusanban, J. Chun, H. Rosen, N.H. Purcell, J.H. Brown, Sphingosine 1-phosphate receptor 3 and RhoA signaling mediate inflammatory gene expression in astrocytes, *J. Neuroinflammation* 14 (1) (2017) 111, <https://doi.org/10.1186/s12974-017-0882-x>.
- [48] H. Kasuya, T. Shimizu, Activated complement components C3a and C4a in cerebrospinal fluid and plasma following subarachnoid hemorrhage, *J. Neurosurg.* 71 (5 Pt 1) (1989) 741–746, <https://doi.org/10.3171/jns.1989.71.5.0741>.
- [49] A. Niwa, K. Osuka, T. Nakura, N. Matsuo, T. Watabe, M. Takayasu, Interleukin-6, MCP-1, IP-10, and MIG are sequentially expressed in cerebrospinal fluid after subarachnoid hemorrhage, *J. Neuroinflammation* 13 (1) (2016) 217, <https://doi.org/10.1186/s12974-016-0675-7>.
- [50] A. Rahmadian, N. Mohebbi, A. Haghnegahdar, E. Kamali Sarvestani, A. Razmkon, J. Kivelev, F. Baghban, Serum levels of monocyte chemoattractant protein-1 correlate with poor clinical grades in cerebral aneurysms, *Iranian J. Immunol.* 12 (4) (2015) 302–310 IJIV12i4A7.
- [51] E. Kooijman, C.H. Nijboer, C.T. van Velthoven, W. Mol, R.M. Dijkhuizen, J. Kesecioglu, C.J. Heijnen, Long-term functional consequences and ongoing cerebral inflammation after subarachnoid hemorrhage in the rat, *PLoS One* 9 (6) (2014) e90584, <https://doi.org/10.1371/journal.pone.0090584>.
- [52] F. Carbone, P.C. Teixeira, V. Braunerreuther, F. Mach, N. Vuilleumier, F. Montecucco, Pathophysiology and treatments of oxidative injury in ischemic stroke: focus on the phagocytic NADPH oxidase 2, *Antioxid. Redox Signal.* 23 (5) (2015) 460–489, <https://doi.org/10.1089/ars.2013.5778>.
- [53] L. Zhang, Z. Li, D. Feng, H. Shen, X. Tian, H. Li, Z. Wang, G. Chen, Involvement of Nox2 and Nox4 NADPH oxidases in early brain injury after subarachnoid hemorrhage, *Free Radic. Res.* 51 (3) (2017) 316–328, <https://doi.org/10.1080/10715762.2017.1311015>.
- [54] Y. Zhan, P.R. Krafft, T. Letic, Q. Ma, R. Souvenir, J.H. Zhang, J. Tang, Imatinib preserves blood-brain barrier integrity following experimental subarachnoid hemorrhage in rats, *J. Neurosci. Res.* 93 (1) (2015) 94–103, <https://doi.org/10.1002/jnr.23475>.